The Enskog theory for self-diffusion coefficients of simple fluids with continuous potentials

K.Miyazaki [1] *, G.Srinivas [2], B.Bagchi [2] †

[1] IRI, Delft University of Technology, 2629 JB Delft, The Netherlands

[2] Solid State and Structural Chemistry Unit, Indian Institute of Science, Bangalore 560 012, India

We develop the Enskog theory for the self-diffusion coefficient for fluids with continuous potentials. General expressions for the memory kernel and the self-diffusion coefficient are derived starting from the Green-Kubo formula. The time-dependent memory kernel is calculated and compared with molecular dynamics simulations for the Lennard-Jones fluid. Excellent agreement is obtained at low density. The self-diffusion coefficient is evaluated for several temperatures and densities. The ratio of the Enskog self-diffusion coefficient to the simulation value is plotted against density for the Lennard-Jones fluid. Significant difference of this density dependence from that for the hard-sphere fluid is observed. In particular, the well-known maximum observed in the hard-sphere fluid is found to be completely absent in the Lennard-Jones fluid.

Key words: *Enskog theory, self-diffusion coefficient, Lennard-Jones fluid, memory kernel*

PACS: *66.30.H, 47.10.+g*

1. Introduction

The well-known Enskog theory for the hard-sphere fluid provides a very good approximation to the transport phenomena in dense gases. Although it is a simple generalization of the Boltzmann equation, its usefulness is beyond dispute. For example, the self-diffusion coefficient calculated from Enskog theory differs by less than 20% from the simulation value [1,2] in the dense gas and low density liquid phase. The Enskog approximation is thus not only practically useful in a wide density range, but it also plays an important role in the mode-coupling theory (MCT)

*E-mail: K.Miyazaki@iri.tudelft.nl
†E-mail: bbagchi@sscu.iisc.ernet.in

[3,4] calculations. As the density increases, each collision of atoms is not independent any more and the ring collisions become important. These effects are taken into account through generalized hydrodynamic modes in the MCT scheme. Most of the input functions necessary to MCT analysis, such as the density correlation function, are usually evaluated using the Enskog theory for the hard-sphere fluid.

However, the Enskog theory, at present, is fully developed only for the hard-sphere fluid and in its present form cannot be applied to more realistic continuous potentials. Considering the usefulness of the Enskog theory for the hard-sphere fluid, it is quite tempting to develop a similar theory for continuous potentials. An Enskog-type theory for the fluids with continuous potentials should be also useful in the calculation of the time-dependent memory kernels whose integration over time provides the transport coefficients. The Enskog-type theory is expected to be a very good approximation to describe the short-time behaviour of the memory kernel because the binary-collisions are dominant dynamical processes at short times. This fact is very important to evaluate the transport coefficient in the high density region under MCT scheme where the knowledge of the short-time dynamics is indispensable. The short-time dynamics depends critically on the details of the intermolecular potential. So far, *ad hoc* fitting functions such as the Gaussian approximation have been used [4,5]. While the Gaussian approximation is satisfactory at very high densities, it fails miserably at low and intermediate densities. Enskog-type theory will provide a much better understanding of the dynamics without any *ad hoc* parameter.

In this paper, we develop an "Enskog theory" for the memory kernel and the self-diffusion coefficient of simple fluids with continuous potentials. Here we shall focus on the Lennard-Jones and soft-core potential.

2. The memory kernels and self diffusion coefficients

We consider an atom in a simple fluid which interacts with other identical atoms with a pairwise potential $\phi(r)$. The frequency-dependent friction coefficient of an atom, $\zeta(z)$, (which is often called the memory kernel) is given by the Green-Kubo formula [3],

$$\zeta(z) = \frac{1}{3k_\mathrm{B}T} \int_0^\infty \mathrm{d}t \ \mathrm{e}^{-zt} \left\langle \boldsymbol{F}(t) \cdot \boldsymbol{F}(0) \right\rangle . \qquad (2.1)$$

Here $\boldsymbol{F}(t)$ is the force between the solute and surrounding solvents at a time t, k_B is the Boltzmann constant and T is the absolute temperature. Note that the integrand in equation (2.1) is not the usual force-force time correlation function. The time evolution of $\boldsymbol{F}(t)$ is driven by a *projected* Liouville operator,

$$\boldsymbol{F}(t) \equiv \exp[\mathrm{i}\mathcal{Q}L_N t]\boldsymbol{F}(0), \qquad (2.2)$$

where $\mathrm{i}L_N$ is the Liouville operator for the N-particle system and $\mathcal{Q} = 1 - \mathcal{P}$ and $\mathcal{P}$ is a projection operator defined by $\mathcal{P} \ast = \left\langle \ast \ v_x \right\rangle v_x / \left\langle v_x^2 \right\rangle$. This equation can be established by using the Mori-Zwanzig projection-operator method [3]. The self-diffusion coefficient D is related to the friction coefficient ζ via the Einstein relation

as $D = k_B T/\zeta$, where $\zeta \equiv \zeta(z = 0)$ is the friction coefficient in the stationary limit. In [6], we have shown that, neglecting all multiple collision contributions, the memory kernel is given by

$$\zeta_E(z) = -\frac{\rho}{3} \sum_{\alpha=x,y,z} \int d\boldsymbol{p} \int d\boldsymbol{r} \; f_0(p) \frac{\partial g(r)}{\partial r_\alpha} \left[z - iL(\mathbf{r}, \mathbf{p})\right]^{-1} \frac{\partial \phi(r)}{\partial r_\alpha}, \qquad (2.3)$$

where ρ is the number density, $\mathbf{r}$ and $\mathbf{p}$ are the relative position and the relative momentum of the two particle system, $f_0(p)$ is the Maxwell distribution function, $g(r)$ is the radial distribution function, and $iL(\boldsymbol{r}, \boldsymbol{p})$ is the Liouville operator for the relative coordinate of the two particle system. The stationary value is obtained by putting $z = 0$ in the above expression and can be given by

$$\zeta_E = \frac{8\rho\sqrt{\pi}}{3(mk_B T)^{3/2}} \int_0^\infty dp \int_0^\infty r^2 dr \int_0^{\pi/2} \sin\theta d\theta \; p_\infty p^2 e^{-p^2/mk_B T} \frac{dg(r)}{dr}$$
$$\times \left\{\cos\left[\chi(p, h, b) - \theta\right] - \cos\left[\chi(p, -h, b) + \theta\right]\right\}, \qquad (2.4)$$

where m is the mass of the atom and $h = r\cos\theta$ and $b = r\sin\theta$ are the parallel and perpendicular distances of the initial position of the two particle system from the collision center. b is often called the impact parameter. p_∞ is the intensity of the momentum at the final state after the collision and given from the energy conservation by $p_\infty = \sqrt{p^2 + m\phi(r)}$. $\chi(p, \pm h, b)$ is the deflection angle which represents the angle formed by the directions between the initial velocity and the velocity at $t = \infty$. The deflection angle can be evaluated from the solution of the equation of motion with the initial condition (p, r, θ) for the momentum and position, respectively.

We may prove that equations (2.3) and (2.4) satisfy the following three important properties.

(i) Equation (2.3) gives the exact initial value for arbitrary density.

$$\zeta_E(t = 0) = \frac{\rho}{3} \int d\boldsymbol{r} \; g(r)\nabla^2\phi(r), \qquad (2.5)$$

which is the well-known expression for the Einstein frequency. This was first shown by Pathak *et al.* [7].

(ii) In the low density limit, equation (2.4) reduces to the familiar Chapman-Enskog expression [8],

$$\zeta_E = \frac{16\rho\sqrt{\pi}}{3(mk_B T)^{3/2}} \int_0^\infty dp \int_0^\infty b \, db \; p^5 e^{-p^2/mk_B T} \left\{1 - \cos\chi(b, p)\right\}. \qquad (2.6)$$

with the deflection angle $\chi(b, p)$ given by

$$\chi(b, p) = \pi - 2b \int_{r_{min}}^\infty dr \; \frac{1}{r^2\sqrt{1 - \frac{m\phi(r)}{p^2} - \frac{b^2}{r^2}}}, \qquad (2.7)$$

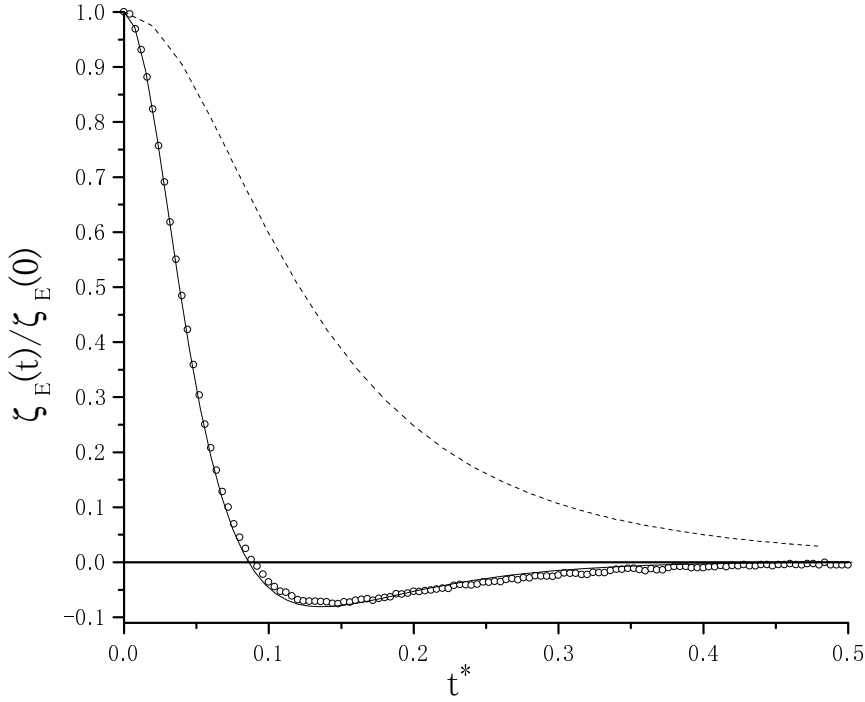where r_{min} is the turning point of the collision process.

Figure 1. $\zeta_{\text{E}}(t)/\zeta_{\text{E}}(0)$ for $T^* = 1.5$, where $t^* = t/\sqrt{m\sigma^2/\epsilon}$ for $\rho^* = 0.1$. The solid line and empty circles are the Enskog calculation and the molecular simulation results given by Yamaguchi *et al.* [9] for the Lennard-Jones fluid, respectively. The dashed line is for the soft-core potential.

(iii) For the hard-sphere potential, we have the well known Enskog expression,

$$\zeta_{\text{E,HS}} = \frac{8}{3}\rho\sigma^2 g(\sigma)\sqrt{m\pi k_{\text{B}}T}, \qquad (2.8)$$

where σ is the radius of the sphere.

Let us now consider the Lennard-Jones potential defined by

$$\phi(r) = 4\epsilon\left\{\left(\frac{\sigma}{r}\right)^{12} - \left(\frac{\sigma}{r}\right)^6\right\}, \qquad (2.9)$$

and the soft-core potential defined by omitting attractive r^{-6} term from the above expression. ϵ and σ are the standard Lennard-Jones parameters. In order to evaluate the memory kernel, one needs the positions at an arbitrary time of all possible trajectories of the two particle system. This is done by solving the equation of motion. $g(r)$ was calculated using the Percus-Yevick closure. The result for $\rho^* = 0.1$ at $T^* = 1.5$ is given in figure 1 for both of the Lennard-Jones and soft-core potentials. The result of the molecular dynamics simulation given by Yamaguchi *et al.* [9] for the Lennard-Jones fluid is also plotted. Here $\rho^* = \rho\sigma^3$ and $T^* = k_{\text{B}}T/\epsilon$. The results are normalized by their initial values. The agreement with the simulation result is excellent for the Lennard-Jones fluid. One observes that the initial fast decay is
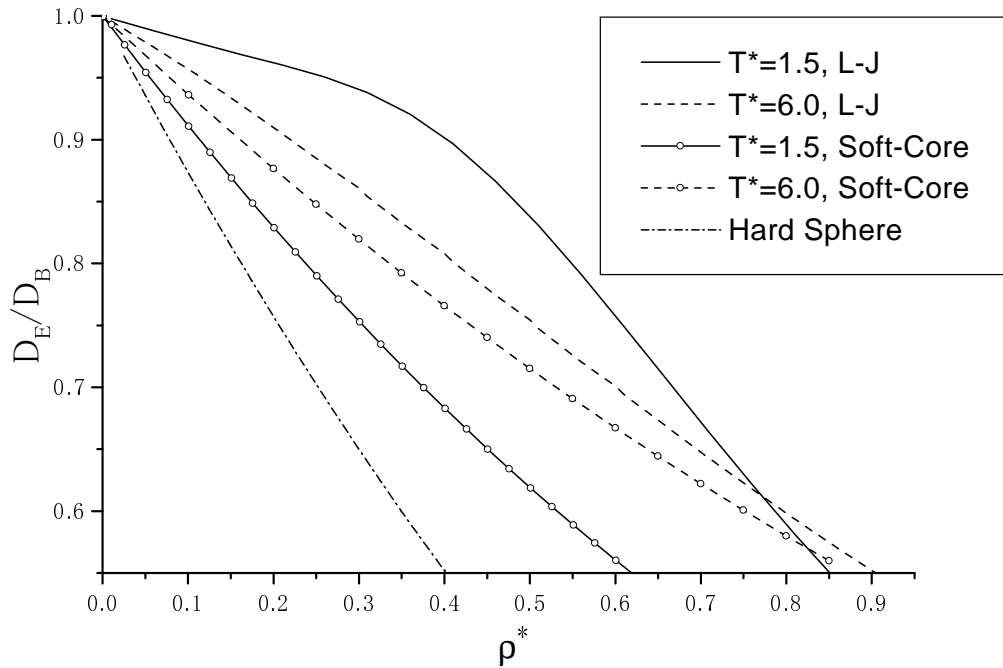
Figure 2. $D_{\mathrm{E}}/D_{\mathrm{B}}$ for the Lennard-Jones and soft-core potentials at $T^* = 1.5$ and 6.0. The result for the hard-sphere fluid is also shown.

followed by a negative tail. This negative dip is due to the attractive part of the potential. This dip is absent in the soft-core fluid.

The self-diffusion coefficient is calculated from equation (2.4) and the Einstein relation $D = k_{\mathrm{B}}T/\zeta$. In figure 2, we plot the density dependence of $D_{\mathrm{E}}/D_{\mathrm{B}}$ for the reduced temperature $T^* = 1.5$ and 6.0. For reference, we also show the Enskog result for the hard-sphere fluid. For the soft-core fluid, we calculated the self-diffusion coefficients for different temperatures using the scaling property which holds for power-low potential fluids,

$$\frac{1}{\sigma}\sqrt{\frac{m}{k_{\mathrm{B}}T}}\, D = T^{*-1/l}F(\rho^* T^{*-3/l}), \tag{2.10}$$

where l is the exponent of the power low potential and $F(x)$ is a scaling function. An important point to note is that the deviation of the Enskog values from the Boltzmann values are always smaller for the continuous potential fluid than those for the hard-sphere fluid. For the soft-core fluid, the line gets closer to the hard-sphere as the temperature gets lower. This is expected because at higher temperatures, the potential becomes effectively less repulsive. On the other hand, for the Lennard-Jones fluid, the slope in the low density gets steeper while the opposite trend is observed in the high density region, as the temperature increases. These tendencies are absent for both the soft-core and the hard-sphere fluid. These results may be rationalized as follows. It is known that $g(r)$ of the Lennard-Jones fluid is influenced
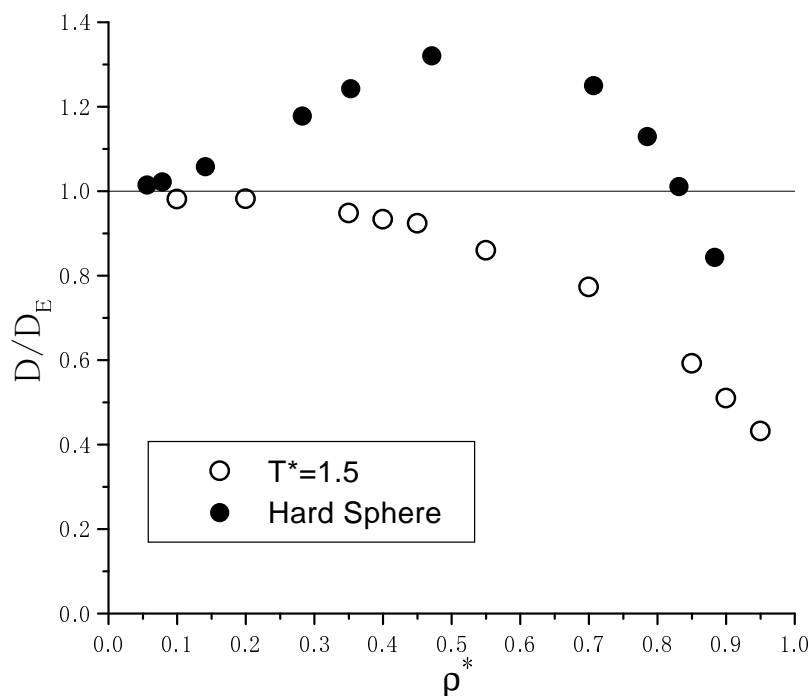
Figure 3. D/D_{E} for $T^* = 1.5$. The empty circles are for the Lennard-Jones fluid at $T^* = 1.5$ [9], The simulation result for hard-sphere fluid is given by filled circles [2].

mostly by the attractive part of the potential in the small density region. As far as the structure in liquid is dominated by the attractive force, $g(r)$ is insensitive to the density. The tendencies are enhanced as the temperature gets lower. This explains the weak dependence of $D_{\mathrm{E}}/D_{\mathrm{B}}$ on the density at low temperatures, as shown in the figure. On the other hand, as the density increases, the repulsive part starts playing a more important role in $g(r)$. In the repulsion dominated region, the structure becomes more hard-sphere like as the temperature goes down. For the larger temperatures, the potential is effectively "softened" and the excluded volume effect becomes smaller, which leads to lower sensitivity of $g(r)$ on the density. This explains the larger density slope for the lower temperature.

In figure 3, we plot the ratio of the self-diffusion coefficient to its Enskog value, D/D_{E}, for the Lennard-Jones fluid at $T^* = 1.5$. The result for the soft-core potential is not shown because of the lack of the simulation data. The hard-sphere result is also plotted. The Enskog theory gives the values closer to the simulation results than the Chapman-Enskog theory at all densities. The figure shows the role of the correlated (and multiple) collisions for the Lennard-Jones potential. In the hard-sphere fluid, one sees an increase of D/D_{E} in the intermediate density followed by the rapid decrease in the high density region. This behaviour can be semi-quantitatively

described by the formula proposed based on the mode-coupling theory [5,10];

$$D = \frac{D_{\mathrm{E}}}{1 + R_\rho} + R_{\mathrm{t}}, \tag{2.11}$$

where R_ρ and R_{t} are the contributions from the coupling of the solute motion to the density and the transverse current fluctuations of the solvents, respectively. In the low density limit, both R_ρ and R_{t} are negligible but as the density increases, the transverse current term R_{t} starts to increase first to give a positive contribution to diffusion. It is due to the back-flow effect where the long-time and long-ranged current fluctuations make a vortex-shaped flow around the atom which enhances diffusion. The decrease at even higher density is attributed to the rapid increase of the density mode contribution, R_ρ in the denominator. The increase in R_ρ indicates a jamming effect on diffusion.

For the Lennard-Jones fluid, however, we do not observe any increase in D/D_{E} in the intermediate density. Instead it decreases monotonically as the density increases. The decrease in the high density region can be explained by the same "caging" scenario as for the hard-sphere fluid. On the other hand, the absence of the increase in D/D_{E} at the intermediate density indicates the absence of any significant back-flow effect. It is surprising because the back-flow originates from the coupling of solute's motion with the long-range hydrodynamic fluctuations and, therefore, it is expected to be insensitive to the details of intermolecular potential.

There could be two obvious explanations for this sensitivity. The first is that the transverse current fluctuation is indeed very sensitive to the shape of the intermolecular potential. R_{t} for the Lennard-Jones fluid might be smaller than that for the hard-sphere fluid, whereas other contributions, D_{E} and R_ρ, remain quantitatively similar for both the potentials. The second scenario is that R_{t} is not much different for both the fluids but $D_{\mathrm{E}}/(1 + R_\rho)$ is much bigger in the Lennard-Jones than in the hard-sphere fluid.

There could be an additional scenario which is a bit more subtle. This involves multiple collisions in fluids for continuous potentials. For hard-sphere potential, the collision is instantaneous and well-defined. The possibility for three or more particles to meet at one time is very small and thus can be simply neglected. Therefore, the deviation from the Enskog values can be attributed to the correlated collisions. For the continuous potentials, however, the definition of a binary collision becomes more ambiguous as the density increases since a third particle could be always there nearby. This multiple collision effect due to the three or more particles is not included in equation (2.11). The similar analysis for the soft-core fluid is desirable to obtain the deeper insight of the reasonings mentioned above.

3. Conclusions

In this paper, a generalization of the Enskog theory for the self-diffusion coefficient and the corresponding memory kernel to fluids with continuous potentials is given. Our starting point is the Green-Kubo formula rather than the conventional

kinetic equation. The expression derived in section 2 can be used for fluids with arbitrary potentials. Advantages of our expression over previous works [7] are that one can relate the Green-Kubo formula to the well-known Chapman-Enskog expression in a straightforward manner in the low density limit and one needs not integrate the memory kernel over time in order to evaluate the self-diffusion coefficient. We evaluated the time-dependent memory kernel and the self-diffusion coefficient for both of the Lennard-Jones and soft-core fluids. For the Lennard-Jones fluid, agreement of the calculated memory kernel with the simulation result is excellent at low density. The self-diffusion coefficient evaluated from our theory was compared with the Chapman-Enskog theory for several densities and temperatures. The result was also compared with simulation result for $T^* = 1.5$ for the Lennard-Jones fluid. It was found that the Enskog theory gives very good agreement. The deviations are within 10% up to $\rho^* = 0.5$. The density dependence of D/D_{E} for the Lennard-Jones fluid is entirely different from that of the hard-sphere fluid. For the Lennard-Jones fluid, there is no increase of D/D_{E} in the intermediate density region which is significant for the hard-sphere fluid. Instead, it exhibits a monotonic decrease. This result might indicate that the effects of correlated and multiple collision to the transport coefficients are very sensitive to the shape of potentials.

Details of the present paper and more systematic comparison with simulation results is found elsewhere [6]

Acknowledgements

References

1. Alder B.J., Wainwright T.E. // Phys. Rev., 1970, vol. 1, p. 18.
2. Erpenbeck J.J., Wood W.W. // Phys. Rev. A, 1991, vol. 43, p. 4254.
3. Boon J.P., Yip S. Molecular Hydrodynamics. New York, Dover, 1980.
4. Balucani U., Zoppi M. Dynamics of the Liquid State. Oxford, Oxford University Press, 1994.
5. Sjögren L., Sjölander A. // J. Phys. C, 1979, vol. 12, p. 4369.
6. Miyazaki K., Srinivas G., Bagchi B. // J. Chem. Phys., 2001, vol. 114, p. 6276.
7. Pathak K.N., Ranganathan S., Johnson R.E. // Phys. Rev. E, 1994, vol. 50, p. 1135.
8. Résibois P., de Leener M. Classical Kinetic Theory of Fluids. New York, Wiley, 1977.
9. Yamaguchi T., Kimura Y., Hirota N. // Mol. Phys., 1998, vol. 94, p. 527.

10. The original expression by Sjögren *et al.* contains additional contributions from other hydrodynamic modes but in the discussion given here, they are not essential.

Теорія Енськога для коефієнтів самодифузії простих флюїдів з неперервними потенціалами

К.Міязакі [1] , Ґ.Срінівас [2] , Б.Багчі [2]

[1] Технологічний університет, 2629 JB Делфт, Нідерданди

[2] Індійський інститут наук, відділ твердого тіла і структурної хімії, Бангалоре 560012, Індія

Теорія Енськога розвивається нами для коефіцієнта самодифузії у флюїдах з неперервними потенціалами. Стартуючи із формули Ґріна-Кубо виведені загальні вирази для ядра пам'яті і коефіцієнта самодифузії. Розраховано залежне від часу ядро пам'яті і проведено порівняння результатів з даними молекулярної динаміки для леннард-джонсівського флюїду. Отримано чудове узгодження при низькій густині. Коефіцієнт самодифузії розрахований для декількох температур і густин. Відношення коефіцієнта самодифузії Енськога до значення, обчисленого з молекулярної динаміки, представлене як функція густини для леннард-джонсівського флюїду. Спостерігається суттєва відмінність густинної залежності від відповідної поведінки у флюїду твердих сфер. Зокрема, добре відомий максимум, що спостерігається у флюїді твердих сфер, повністю відсутній у леннард-джонсівському випадку.

Ключові слова: *теорія Енськога, коефіцієнт самодифузії, леннард-джонсівський флюїд, ядро пам'яті*

PACS: *66.30.H, 47.10.+g*